Journal of Sound and Vibration (2002) **258**(5), 829–845
doi:10.1006/jsvi.2002.5152, available online at http://www.idealibrary.com on IDEAL®

EXPERIMENTAL VALIDATION OF THE CONSTANT LEVEL METHOD FOR IDENTIFICATION OF NON-LINEAR MULTI-DEGREE-OF-FREEDOM SYSTEMS

G. Dimitriadis

*School of Engineering, The University of Manchester, Oxford Road, Manchester M*13 9*PL, England.*
E-mail: grigorios.dimitriadis@man.ac.uk

(*Received* 19 *November* 2001, *and in final form* 5 *February* 2002)

System identification for non-linear dynamical systems could find use in many applications such as condition monitoring, finite element model validation and determination of stability. The effectiveness of existing non-linear system identification techniques is limited by various factors such as the complexity of the system under investigation and the type of non-linearities present. In this work, the constant level identification approach, which can identify multi-degree-of-freedom systems featuring any type of non-linear function, including discontinuous functions, is validated experimentally. The method is shown to identify accurately an experimental dynamical system featuring two types of stiffness non-linearity. The full equations of motion are also extracted accurately, even in the presence of a discontinuous non-linearity.

1. INTRODUCTION

System identification has important applications in many engineering fields, such as modal analysis, control system design and condition monitoring. The main purpose of most system identification techniques is to develop a mathematical model that fully describes a given system. This mathematical model can be used to explain the behaviour of the system and to predict its response to various inputs at different conditions.

During the last couple of decades, system identification for non-linear systems has become of increasing importance. It is now widely accepted that many, if not most, engineering systems and processes are non-linear and that their dynamics cannot be fully captured using linear identification techniques. Hence a number of system identification methods for nonlinear systems have been proposed such as the NARMAX model [1], Volterra series representations [2], Hilbert Transform techniques [3], higher order spectra [4] and the restoring force method [5], which can identify non-linear dynamic systems given sets of inputs and outputs. Neural network [6] and proper orthogonal decomposition based [7] approaches have also been proposed. However, these methods are very complex, difficult to apply and they are not universally valid. For instance, both NARMAX and the higher order spectra method are incapable of identifying systems with discontinuous non-linearities, such as bilinear stiffness or freeplay, which are common in vibrating engineering systems. Additionally, in spite of a number of developments and refinements [8,9], the application of the restoring force to multi-degree-of-freedom systems is still problematic.

A very important consideration for any identification of dynamic systems concerns the form of the resulting mathematical model, which can be either parametric or non-

0022-460X/02/$35.00

parametric [10]. Parametric models contain exclusively terms with physical meaning which reflect the true character of the system under investigation. Hence, they are preferable for the purpose of analyzing and characterizing the behaviour of a given system. Nevertheless, NARMAX models and restoring force surfaces usually contain both parametric and non-parametric terms. Neural networks are exclusively non-parametric, hence, models obtained using these methods contain terms without any physical meaning.

Consequently, there is still a need for a simple, easy to use identification method for nonlinear systems which can identify systems with many degrees of freedom, continuous and discontinuous non-linear components and create parametric models. Such a method is the constant level identification (CLI) approach for the identification of non-linear dynamical systems [11]. The method is a development of the restoring force technique, adapted to identify the non-linearity present in a single- or multi-degree-of-freedom system without the need for curve fitting. The method is flexible enough to be able to deal with a large class of non-linear systems and functions. Its main limitation is the fact that it can only deal with systems containing non-linear functions which depend on only one of the system state variables. As a consequence, the method is considered more suitable for dynamic systems which contain a single dominant non-linearity, such as the all-moveable tail surfaces of combat aircraft [12]. However, the method has only been demonstrated on simulated systems. In this paper, CLI is employed to identify two experimental systems with two different non-linear functions, namely cubic and bilinear stiffness. The purpose of this demonstration is to validate the CLI technique on real data and to demonstrate its effectiveness on systems featuring both continuous and discontinuous non-linearities.

First, the mathematical basis of the method will be briefly explained, and then the experimental results will be presented.

2. MATHEMATICAL BASIS OF CLI

Linear dynamical systems are usually described by the general equation

$$\mathbf{M}\ddot{\mathbf{q}} + \mathbf{C}\dot{\mathbf{q}} + \mathbf{K}\mathbf{q} = \mathbf{F}(t), \tag{1}$$

where $\mathbf{M}$, $\mathbf{C}$ and $\mathbf{K}$ are the mass, damping and stiffness matrices, respectively, $\mathbf{q}$ is the displacement vector and $\mathbf{F}$ is the excitation force vector. Non-linear systems will, in general, contain stiffness and damping non-linearities. For such systems, a more general set of equations can be defined

$$\mathbf{M}\ddot{\mathbf{q}} + \mathbf{f}(\dot{\mathbf{q}}, \mathbf{q}) = \mathbf{F}(t), \tag{2}$$

where $\mathbf{f}(\dot{\mathbf{q}}, \mathbf{q})$ is the restoring force of the system and can be a linear or a non-linear function.

The CLI method, whilst maintaining the flexibility of the restoring force method to be able to deal with all types of non-linearity, avoids the difficulties associated with the application of the latter approach to multi-degree-of-freedom systems. Use is made of the fact that, if the non-linear function depends on only one of the state variables then, at an arbitrary response level, the restoring force due to the non-linearity is constant. The approach estimates the exact equation of motion of the system by curve-fitting the response at this chosen response level.

The first crucial aspect of the CLI method is to multiply the equations of motion throughout by the inverse of the mass matrix, so that the mass matrix is no longer a quantity that needs to be identified. The restoring force equation becomes

$$\ddot{\mathbf{q}} + \mathbf{M}^{-1}\mathbf{f}(\mathbf{x}) = \mathbf{M}^{-1}\mathbf{F}, \tag{3}$$

where $\mathbf{x}$ is the state vector, given by $\mathbf{x} = [\dot{\mathbf{q}}\ \mathbf{q}]^{\mathrm{T}}$ and now $\mathbf{M}^{-1}\mathbf{F}$ must also be treated as an unknown. The crucial assumption behind the CLI method is that the restoring force function $\mathbf{f}(\mathbf{x})$ has linear components and that the non-linear components depend on *only one* of the state variables, say the ith component, x_i. Then, $\mathbf{f}(\mathbf{x})$ can be re-written as

$$\mathbf{f}(\mathbf{x}) = \mathbf{L}[\, x_1 \ldots x_{i-1} \quad x_{i+1\ldots} x_{2m}\,]^{\mathrm{T}} + \mathbf{g}(x_i),$$

where m is the number of modes (or degrees of freedom) of the system, $\mathbf{L}$ is a constant matrix coefficient of size $m \times (2m-1)$ and $\mathbf{g}(x_i)$ is a $m \times 1$ vector of linear and/or non-linear functions which depend only on x_i. Then, equation (3) becomes

$$\ddot{\mathbf{q}} + \mathbf{M}^{-1}\mathbf{L}[\, x_1 \ldots x_{i-1} \quad x_{i+1\ldots} x_{2m}\,]^{\mathrm{T}} + \mathbf{M}^{-1}\mathbf{g}(x_i) = \mathbf{M}^{-1}\mathbf{F} \tag{4}$$

keeping in mind that this equation, and hence the CLI method, only applies to systems where the non-linearity really is a function of only one state variable. One final adjustment is to write $\mathbf{M}^{-1}\mathbf{F}(t)$ as $\mathbf{M}^{-1}\mathbf{A}\mathbf{w}(t)$ where $\mathbf{w}(t)$ is the $p \times 1$ vector of the measured inputs to the system, $\mathbf{A}$ is a $m \times p$ vector of constant amplitudes and $\mathbf{F}(t) = \mathbf{A}\mathbf{w}(t)$. Hence, the governing equation of the CLI approach is obtained as

$$\ddot{\mathbf{q}} + \mathbf{M}^{-1}\mathbf{L}[\, x_1 \ldots x_{i-1} \quad x_{i+1\ldots} x_{2m}\,]^{\mathrm{T}} + \mathbf{M}^{-1}\mathbf{g}(x_i) = \mathbf{M}^{-1}\mathbf{A}\mathbf{w}(t). \tag{5}$$

Given measurements of $\ddot{\mathbf{q}} \cdot \dot{\mathbf{q}} \cdot \mathbf{q}$ and $\mathbf{w}$ at times t_j where x_i is a constant, equation (5) can be expanded in order to solve for the unknown constants $\hat{\mathbf{L}} = \mathbf{M}^{-1}\mathbf{L}$, $\mathbf{N} = \mathbf{M}^{-1}\mathbf{g}(x_i)$ and $\hat{\mathbf{A}} = \mathbf{M}^{-1}\mathbf{A}$. Expanding for all times t_j, equation (5) becomes

$$\begin{pmatrix} x_1(t_1) & \ldots & x_{i-1}(t_1) & x_{i+1}(t_1) & \ldots & x_{2m}(t_1) & w_1(t_1) & \ldots & w_p(t_1) & 1 \\ x_1(t_2) & \ldots & x_{i-1}(t_2) & x_{i+1}(t_2) & \ldots & x_{2m}(t_2) & w_1(t_2) & \ldots & w_p(t_2) & 1 \\ \vdots & \vdots & \vdots & \vdots & \vdots & \vdots & \vdots & \vdots & \vdots & \vdots \\ x_1(t_n) & \ldots & x_{i-1}(t_n) & x_{i+1}(t_n) & \ldots & x_{2m}(t_n) & w_1(t_n) & \ldots & w_p(t_n) & 1 \end{pmatrix} \begin{Bmatrix} \hat{L}_{k,1} \\ \vdots \\ \hat{L}_{k,2m-1} \\ \hat{A}_{k,1} \\ \vdots \\ \hat{A}_{k,p} \\ N_k \end{Bmatrix}$$

$$= \begin{Bmatrix} \ddot{q}_k(t_1) \\ \ddot{q}_k(t_2) \\ \vdots \\ \ddot{q}_k(t_n) \end{Bmatrix} \tag{6}$$

for $k = 1, \ldots, m$ and where n is the total number of time instances t_j. Equation (6) can be solved to obtain every line of $\hat{\mathbf{L}}$, $\mathbf{N}$ and $\hat{\mathbf{A}}$ separately. Hence, each of the m equations of motion is also identified separately. Equation (6) also demonstrates an additional advantage of multiplying throughout by the inverse of the mass matrix, namely that the number of unknowns is reduced, speeding up the computation and also improving the accuracy of the fit.

At the time instances t_j where x_i is a constant, $\mathbf{N}$ is also a constant. However, at a general time instance, t, $\mathbf{N} = \mathbf{N}(t)$. The variation of $\mathbf{N}$ with time can be obtained once $\hat{\mathbf{L}}$, $\mathbf{N}(t_j)$ and $\hat{\mathbf{A}}$ have been evaluated by re-writing equation (5) as

$$\mathbf{N}(t) = -\ddot{\mathbf{q}} - \hat{\mathbf{L}}[\, x_1 \ldots x_{i-1} \quad x_{i+1} \ldots x_{2m}\,]^{\mathrm{T}} + \hat{\mathbf{A}}w(t). \tag{7}$$

The end result of the CLI procedure is the complete identification of the equations of motion of a given system in the form

$$\ddot{\mathbf{q}} + \hat{\mathbf{L}}[\, x_1 \ldots x_{i-1} \quad x_{i+1} \ldots x_{2m}\,]^{\mathrm{T}} + \mathbf{N}(t) = \hat{\mathbf{A}}\mathbf{w}(t). \tag{8}$$

Now define $\hat{\mathbf{C}} = \mathbf{M}^{-1}\mathbf{C}$ and $\hat{\mathbf{K}} = \mathbf{M}^{-1}\mathbf{K}$. Then $\hat{\mathbf{L}} = [\,\hat{\mathbf{C}} \quad \hat{\mathbf{K}}\,]$, but where either $\hat{\mathbf{C}}$ or $\hat{\mathbf{K}}$ is missing a column. The missing linear information is imbedded in $\mathbf{N}(t)$ together with the non-linear information. Plotting $\mathbf{N}(t)$ against $x_i(t)$ will yield the shape of the non-linearity added to the linear term missing from $\hat{\mathbf{L}}$.

The following considerations need to be taken into account when using the CLI approach:

- The number of modes, m, may not be known for a real system. In the case of mildly non-linear systems, preliminary analysis could give an indication of the number of modes via frequency response function (FRF) plots.
- The location of non-linearities present in the system may not be known in advance. This can be obtained using a Hilbert transform approach [13]. Alternatively, the CLI approach can be applied speculatively, i.e., each one of the state variables is assumed to contain the non-linearity. The CLI technique is then applied for each case. The correct case is when plots of $\mathbf{N}(t)$ against $x_i(t)$ are obtained which are single-valued functions. If no such case exists, then the non-linearity present in the system depends on more than one of the system variables and the CLI method cannot be applied.
- In order for the identification process to succeed, the input and output data need to be interpolated to obtain a set of instances in time where the desired variable, $x_i(t)$, has exactly the same value, say $x_i = c$. Cubic interpolation has been found quite adequate. The choice of the value of c is quite important since, by choosing $c = 0$, a large amount of measurement noise will be included in the identification process. Conversely, if $c = \max(x_i)$ then there will not be enough points to solve equations (6). A practical choice for the identification level is $c = \sqrt{\overline{x_i^2}}$. Nevertheless, the choice of c is usually dictated by the signal-to-noise ratio of $x_i(t)$. The lower this ratio, the higher value of c must be in order to attempt to minimize the amount of measurement noise included in the identification process.
- A further consideration regarding the CLI method concerns the effect of performing the identification procedure at various levels, i.e., applying equation (6) at times t_j, where $x_i = c_1, c_2, \ldots$, where c_1, c_2, etc., are various constant values. In the case where a significant amount of noise is present in the response data, identified models obtained using a low constant level will be highly suspect because the noise may create artificial crossings of that level. In these cases, additional identifications must be carried out at higher constant levels in order to check to what degree the identified model is biased by noise. In other words, to ensure that the constant level at which the identification process is carried out is the optimum, a number of levels must be tried out and the level that yields the least biased model must be chosen. Applications of the CLI method to simulated systems have shown that, using multiple identification levels, the non-linear function is correctly identified for a signal-to-noise ratio of up to approximately 0·5.
- The excitation force also needs to be such that it excites all the important features of the systems, including the non-linearity. Sine-sweep or banded random excitation signals are suitable, since they allow several frequencies of excitation to be applied to the system in one test.
- The CLI technique can also work for systems where the non-linear functions depend on a single combination of more than one state variable, e.g., $g(x_2 - x_1)$. In this case, the

identification is performed at time instances where the value of $x_2(t) - x_1(t)$ is a constant.

It should be noted that the non-linearities identified by the method need not be single-valued functions. Hysteresis-type non-linearities can also be identified [11] but, if such a non-linearity is expected, then the procedure needs to be applied on constant values of x_i with only positive or only negative derivative.

3. EXPERIMENTAL VALIDATION

The CLI method is here demonstrated on a 2-degree-of-freedom (d.o.f.) mass–spring dynamical system. A photograph of the experimental set-up is shown in Figure 1. Figure 2 shows an idealized diagram of the experimental set-up. The rig consisted of two masses (M_1 and M_2) independently supported by a couple of cantilever steel plates with stiffnesses K_1 and K_2. The two masses were attached to each other by a coupling spring with stiffness K_{12}. Each mass was independently excited by means of a shaker driven by a signal generator, the excitation signals F_1 and F_2 being measured by means of a force gauge. The excitation signals used for the experiment were random with a flat spectrum between 10 and 30 Hz. One accelerometer on each mass measured the accelerations a_1 and a_2, which were then integrated to obtain the displacements y_1 and y_2. The time duration of the tests was 4·095 s and the sampling interval 0·001 s.

For the non-linear spring, K_{NL}, three different configurations were tested:

- Linear ($K_{NL} = 0$)
- Cubic spring attached to mass 2. The cubic spring was chosen as an example of a continuous non-linear function.
- Freeplay spring attached to mass 2, leading to a bilinear stiffness since the mass remained attached to the linear cantilever plates. The bilinear stiffness was chosen as an example of a discontinuous non-linear function.

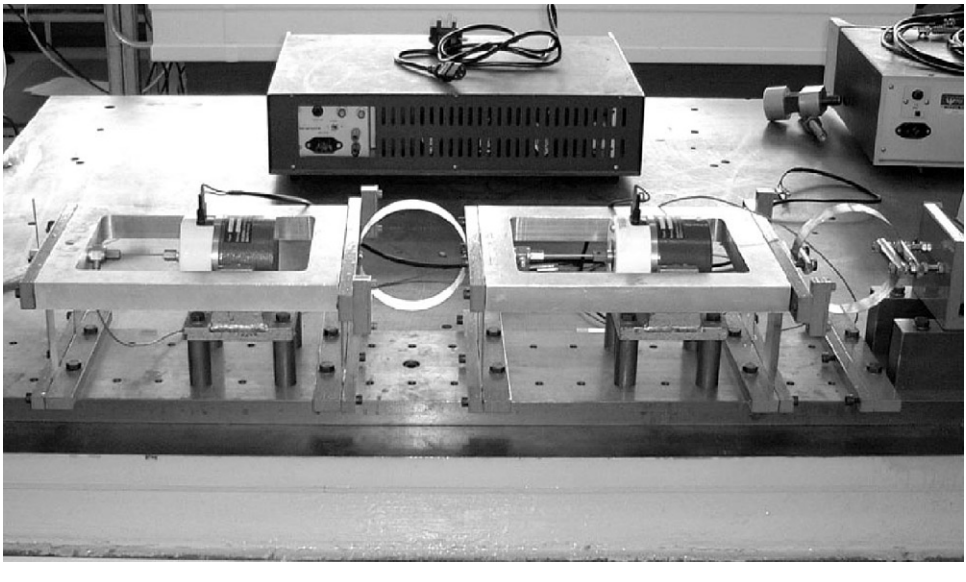

Figure 1. Picture of experimental set-up.

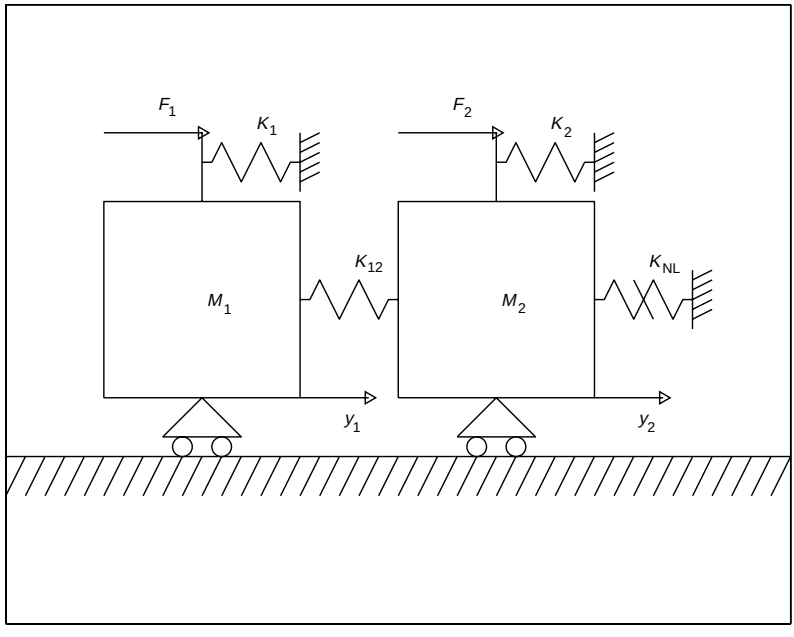

Figure 2. Idealized drawing of experimental set-up.

The cubic stiffness was implemented by means of a steel ruler under transverse loading and the freeplay by means of a steel ring moving between two pegs separated by a distance δ. It should be noted that the cubic experiments were carried out on a slightly different system to the one on which the linear and bilinear tests were carried out. Specifically, the basic rig was the same but, in the case of the cubic experiments, there were four cantilever plates supporting each mass while, in the case of the linear and bilinear experiments, there were only two cantilever plates. Additionally, during the cubic experiments, the forces applied to the two masses were not forced to be of the same amplitude. As a result, the identified matrices for the cubic system are significantly different to those for the linear and bilinear systems. Nevertheless, all of the experiments were suitable for the validation of the CLI method. For all the applications of the CLI technique described below, the chosen constant level was equal to the root-mean-square value of the relevant signal.

3.1. IDENTIFICATION OF LINEAR SYSTEM

The linear system was identified using standard frequency domain analysis techniques based on the curve fitting of the FRF as well as the CLI method. It should be noted that the CLI procedure is inefficient when applied to linear systems since it assumes non-linearity, however, it does yield an accurate identification. The FRF results revealed that the linear system has two natural frequencies at 15·5 and 24·7 Hz.

In order to apply the CLI approach, measurements of acceleration, displacement and velocity are required. As the responses of the 2-d.o.f. system were measured using accelerometers, only acceleration data were available. The velocity and displacement responses were obtained by integrating the acceleration data in the frequency domain. In order to eliminate drift in the integrated signals, the Fourier transforms of the

accelerations were set to zero at frequencies below 5 Hz. Additionally, the input signals were designed as 95% bursts in order to avoid leakage.

The CLI technique was applied to the linear system assuming that there was a non-linear function depending on the displacement of the second mass, y_2. The resulting damping and stiffness matrices were

$$\hat{\mathbf{C}} = \begin{bmatrix} 2{\cdot}7230 & -0{\cdot}7400 \\ -0{\cdot}6407 & 3{\cdot}2747 \end{bmatrix}, \quad \hat{\mathbf{K}} = 10^4 \begin{bmatrix} 1{\cdot}0996 & 0 \\ -0{\cdot}2798 & 0 \end{bmatrix}, \quad \hat{\mathbf{A}} = \begin{Bmatrix} 0{\cdot}3475 & 0{\cdot}0000 \\ 0{\cdot}0000 & 0{\cdot}3350 \end{Bmatrix}. \quad (9)$$

Note $\hat{\mathbf{K}}$ contains zeroes in the second column since that column represents y_2. Also note that matrix $\hat{\mathbf{A}}$ is diagonal and that its two diagonal elements are almost equal, which was expected since there were only two input signals with the same amplitude. Then, equation (7) was applied to obtain the variation of $\mathbf{N}$ with y_2, which is shown in Figure 3. Note that both components of $\mathbf{N}$ are linear, denoting that the system is linear. By measuring the slope of the two lines, the stiffness matrix could be completed:

$$\hat{\mathbf{K}} = 10^4 \begin{bmatrix} 1{\cdot}0996 & -0{\cdot}3152 \\ -0{\cdot}2798 & 1{\cdot}5863 \end{bmatrix}.$$

Note that reciprocity is approximately satisfied since the stiffness matrix is nearly symmetric. The full equations of motion of the linear system were then obtained as

$$\begin{bmatrix} 1 & 0 \\ 0 & 1 \end{bmatrix} \begin{Bmatrix} \ddot{y}_1 \\ \ddot{y}_2 \end{Bmatrix} + \begin{bmatrix} 2{\cdot}7320 & -0{\cdot}7400 \\ -0{\cdot}6407 & 3{\cdot}2747 \end{bmatrix} \begin{Bmatrix} \dot{y}_1 \\ \dot{y}_2 \end{Bmatrix} + 10^4 \begin{bmatrix} 1{\cdot}0996 & -0{\cdot}3152 \\ -0{\cdot}2798 & 1{\cdot}5863 \end{bmatrix} \begin{Bmatrix} y_1 \\ y_2 \end{Bmatrix} = \begin{Bmatrix} 0{\cdot}3475 w_1(t) \\ 0{\cdot}3350 w_2(t) \end{Bmatrix}.$$

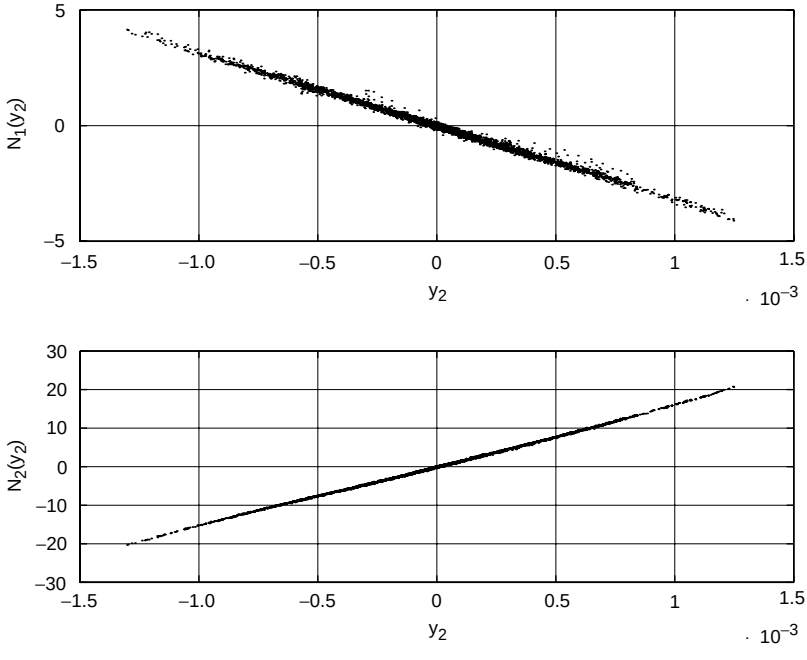

Figure 3. $\mathbf{N}(y_2)$ (N) against y_2 (m) for linear system.

The eigenfrequencies of the identified system of equations were found to be 15·6 and 20·9 Hz, i.e., very close to the values obtained from the FRF analysis (15·5 and 20·7 Hz). Hence, the CLI identification of the linear system was successful. A final check of the validity of the identified equations was performed by applying the same excitation forces to both the real system and the identified model and then comparing the resulting acceleration signals. The identified equations of motion were integrated numerically using a Runge–Kutta approach to yield the response to the chosen excitation signals. A portion of the acceleration signals of mass 2 is plotted in Figure 4. The two signals are almost identical.

3.2. IDENTIFICATION OF SYSTEM WITH CUBIC STIFFNESS

A cubic spring was attached to mass 2 in the form of a steel ruler under transverse loading. The CLI method was applied to randomly forced response data from the experimental rig. Figures 5 and 6 show the identified $N_1(y_2)$ and $N_2(y_2)$ term variation plotted against the displacement of mass 2. The curve in Figure 5 is still linear but Figure 6 shows a slightly cubic variation. The identified matrices were:

$$\hat{\boldsymbol{C}} = \begin{bmatrix} 5{\cdot}5302 & -0{\cdot}4777 \\ -0{\cdot}4023 & 4{\cdot}1891 \end{bmatrix}, \quad \hat{\mathbf{K}} = 10^4 \begin{bmatrix} 2{\cdot}2825 & 0 \\ -0{\cdot}3093 & 0 \end{bmatrix}, \quad \begin{Bmatrix} 1{\cdot}5603 & 0{\cdot}0000 \\ 0{\cdot}0000 & 2{\cdot}7629 \end{Bmatrix}.$$

As in the linear case, the equations of motion were completed by curve fitting the variation of $\mathbf{N}$ with y_2. Since, $N_1(y_2)$ is linear (see Figure 5), it was curve fitted by a first degree

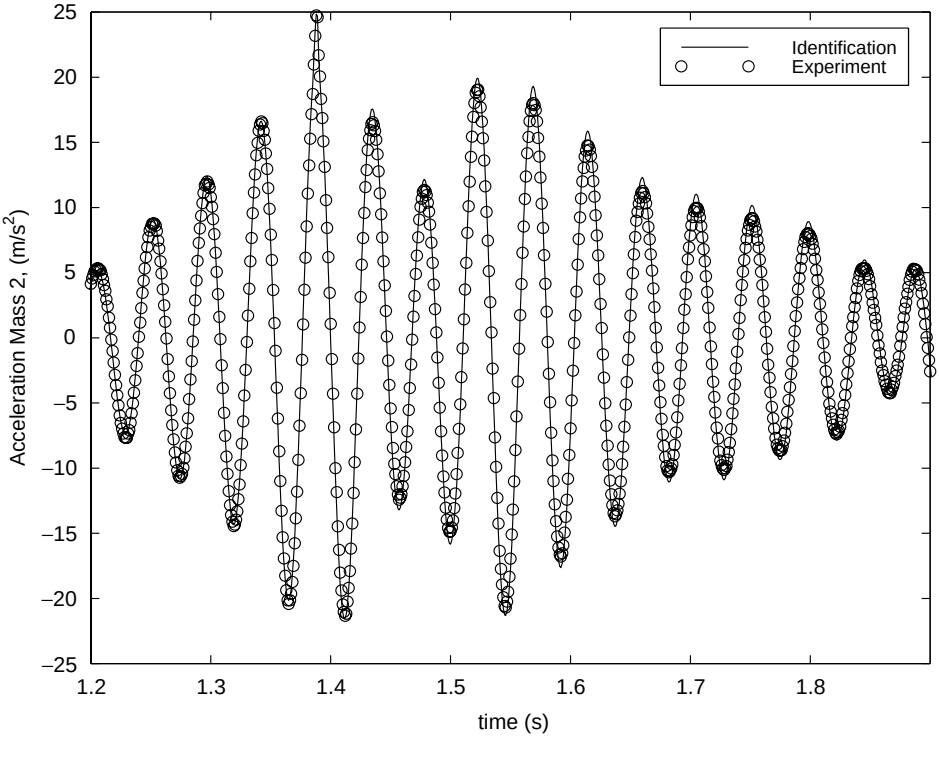

Figure 4. Comparison of response from real system and identified model. ——, Identification; ○—○, experiment.

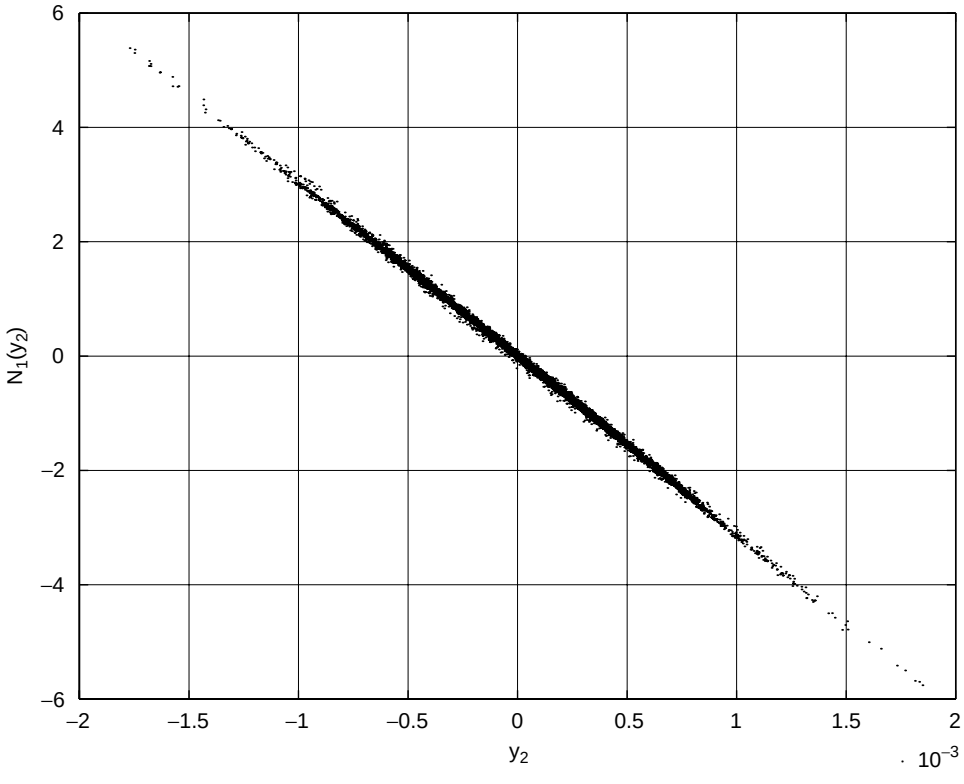

Figure 5. $N_1(y_2)$ (N) against y_2 (m) for system with cubic stiffness.

polynomial. The resulting polynomial was

$$N_1(y_2) = -0{\cdot}3081 \times 10^4 y_2 - 0{\cdot}0184. \tag{10}$$

Note that the first order coefficient, $0{:}381 \times 10^4$, is approximately equal to the $K(2,1)$ term, thus satisfying reciprocity. $N_2(y_2)$ was estimated by curve fitting Figure 6 by a cubic polynomial:

$$N_2(y_2) = 1{\cdot}3036 \times 10^9 y_2^3 + 5{\cdot}7876 \times 10^5 y_2^2 + 2{\cdot}2555 \times 10^4 y_2 - 0{\cdot}1067. \tag{11}$$

The displacement y_2 is of order $O(10^{-3})$ and $N_2(y_2)$ is of order $O(10)$. The terms in equation (11) are of order:

$$y_2^3 : O(1), \quad y_2^2 : O(10^{-1}), \quad y_2^1 : O(10), \quad y_2^0 : O(10^{-1}).$$

Hence, the zeroth and second order terms can be neglected and, since the first order term is due to the linear cantilever springs, the cubic stiffness caused by the steel ruler is given by $K_{cubic} = 1{\cdot}3 \times 10^9 y_2^3$. After substituting for term $\hat{K}_{1,2}$ the slope of equation (10) and for $\hat{K}_{2,2}$, the first order coefficient of equation (11), the equations of motion were obtained as

$$\begin{bmatrix} 1 & 0 \\ 0 & 1 \end{bmatrix} \begin{Bmatrix} \ddot{y}_1 \\ \ddot{y}_2 \end{Bmatrix} + \begin{bmatrix} 5{\cdot}5302 & -0{\cdot}4777 \\ -0{\cdot}4023 & 4{\cdot}1891 \end{bmatrix} \begin{Bmatrix} \dot{y}_1 \\ \dot{y}_2 \end{Bmatrix} + 10^4 \begin{bmatrix} 2{\cdot}2825 & -0{\cdot}3081 \\ -0{\cdot}3093 & 2{\cdot}2555 \end{bmatrix} \begin{Bmatrix} y_1 \\ y_2 \end{Bmatrix}$$
$$+ \begin{Bmatrix} 0 \\ 1{\cdot}3036 \times 10^9 y_2^3 \end{Bmatrix} = \begin{Bmatrix} 1{\cdot}5603 w_1(t) \\ 2{\cdot}7629 w_2(t) \end{Bmatrix}. \tag{12}$$

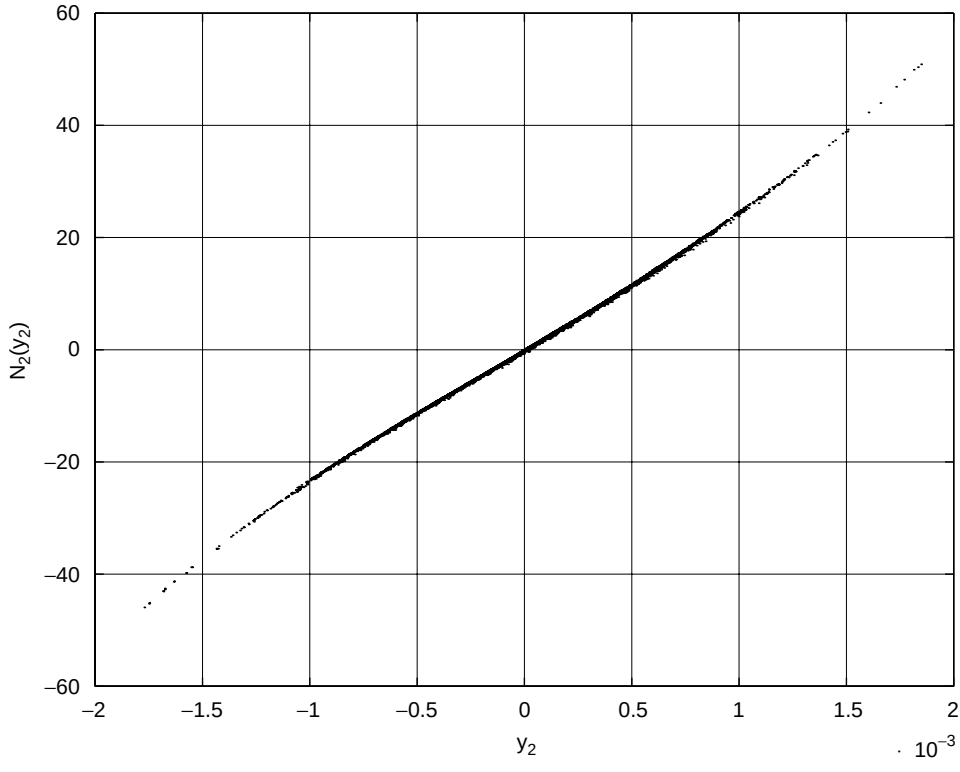

Figure 6. $N_2(y_2)$ (N) against y_2 (m) for system with cubic stiffness.

This set of equations was verified by calculating its response to the same excitation signals that were used on the experimental system. Figure 7 compares the accelerations obtained from the identified equations and the actual system. It is obvious that the comparison is very favourable.

3.3. IDENTIFICATION OF SYSTEM WITH BILINEAR STIFFNESS

A freeplay spring was attached to mass 2 in the form of a steel ring moving between two restraining pegs at a distance δ apart. Mass 2 was still supported on the cantilever plates and, hence, the resulting combined spring attached to mass 2 was bilinear. The CLI method was applied to randomly forced response data from the experimental rig. Two cases were investigated, one where $\delta = 0{\cdot}5$ mm and one where $\delta = 1{\cdot}05$ mm. The excitation amplitudes for the two cases were equal.

It should be noted here that, due to the design of the freeplay spring, the measured acceleration signals exhibited quite a lot of rattling. The rattling was caused by the fact that the steel ring was not perfectly parallel to the two pegs resulting in repeated impacts of the ring on the pegs. A sample of the acceleration signals is shown in Figure 8. The rattling behaviour was more apparent in the $\delta = 0{\cdot}5$ mm case because the steel ring was impacting on the pegs at higher velocities than in the $\delta = 1{\cdot}05$ mm case. Nevertheless, the integration process smoothed out the rattling effect on the calculated velocity and displacement signals, since integration is a form of averaging. Hence, a part of the non-linear behaviour

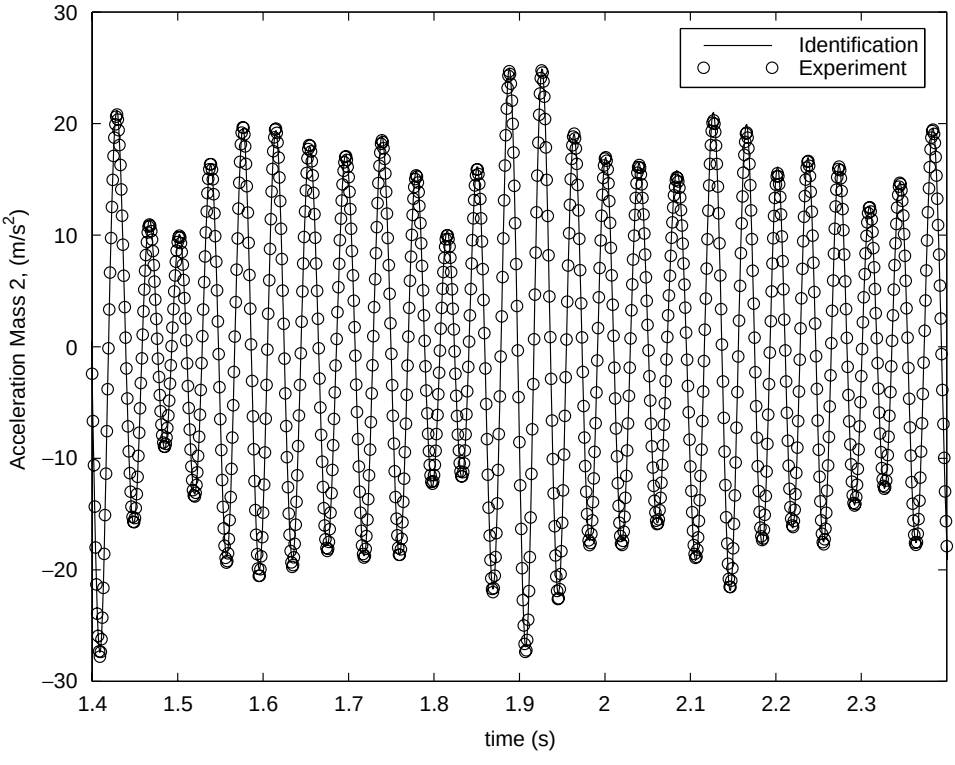

Figure 7. Comparison of experimental and identified responses for system with cubic stiffness. ——, Identification; ○—○, experiment.

of the experimental system was not captured by the identification process. In order to identify the rattling behaviour, velocity and displacement sensors would have been required in addition to the accelerometers.

The identified matrices for the $\delta = 0{\cdot}5$ mm case were:

$$\hat{\mathbf{C}} = \begin{bmatrix} 2{\cdot}7564 & -0{\cdot}4500 \\ -0{\cdot}4791 & 3{\cdot}6802 \end{bmatrix}, \quad \hat{\mathbf{K}} = 10^4 \begin{bmatrix} 1{\cdot}0833 & 0 \\ -0{\cdot}2810 & 0 \end{bmatrix}, \quad \hat{\mathbf{A}} = \begin{Bmatrix} 0{\cdot}3472 & 0{\cdot}0000 \\ 0{\cdot}0000 & 0{\cdot}3288 \end{Bmatrix}.$$

The identified matrices for the $\delta = 1{\cdot}05$ mm case were:

$$\hat{\mathbf{C}} = \begin{bmatrix} 2{\cdot}7471 & -0{\cdot}6596 \\ -0{\cdot}6093 & 3{\cdot}8485 \end{bmatrix}, \quad \hat{\mathbf{K}} = 10^4 \begin{bmatrix} 1{\cdot}1006 & 0 \\ -0{\cdot}2795 & 0 \end{bmatrix}, \quad \hat{\mathbf{A}} = \begin{Bmatrix} 0{\cdot}3486 & 0{\cdot}0000 \\ 0{\cdot}0000 & 0{\cdot}3303 \end{Bmatrix}.$$

In both cases, all the identified matrices are approximately equal to the matrices of the linear system, showing that the bilinear stiffness only affects $\mathbf{N}(y_2)$. The off-diagonal damping terms for the $\delta = 0{\cdot}5$ mm appear to be slightly lower than the corresponding terms obtained from the linear and $\delta = 1{\cdot}05$ mm.

The plots of $N_1(y_2)$ against y_2 for both cases were linear, as in the cubic stiffness example. Their slopes where $\hat{\boldsymbol{K}}_{1,2} = -3{\cdot}1797 \times 10^3$ for $\delta = 0{\cdot}5$ mm and $\hat{\boldsymbol{K}}_{1,2} = -3{\cdot}1209 \times 10^{-4}$ for $\delta = 1{\cdot}05$ mm.

Figures 9 and 10 show the identified non-linear term, $N_2(y_2)$, variation for each case, respectively, plotted against the displacement of mass 2. Figure 9 shows the force–displacement plot for the $\delta = 0{\cdot}5$ mm case. By curve fitting the plot, it was found that there

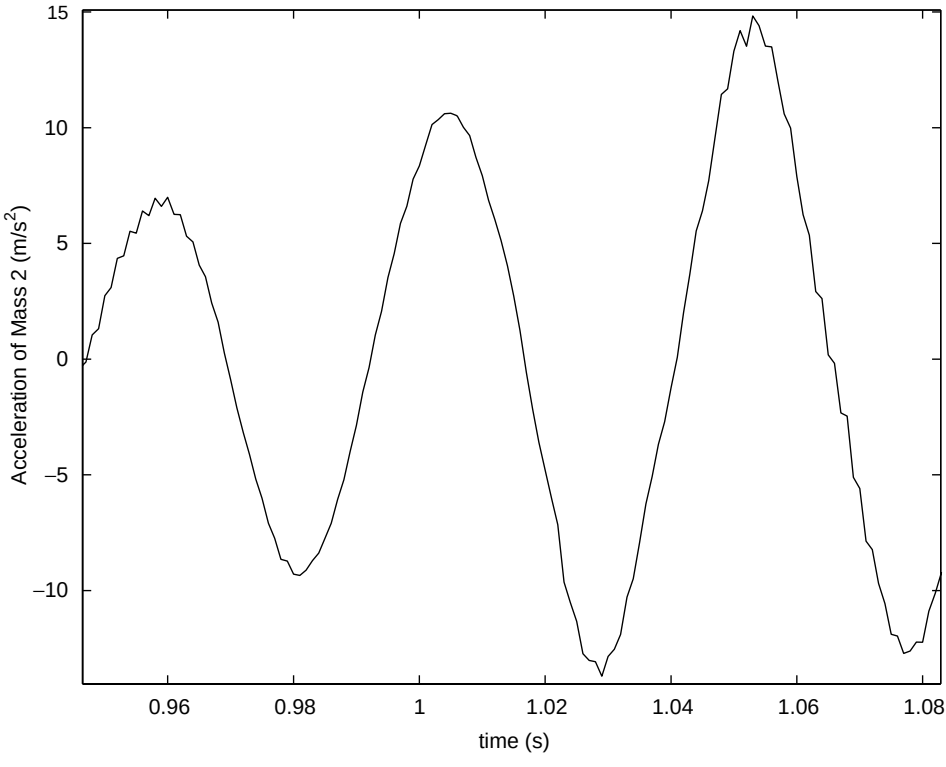

Figure 8. Section of measured acceleration signal from system with stiffness spring displaying rattling behaviour.

are three piecewise-linear stiffnesses, the values of which are

$$K_{out,left} = 1{\cdot}9047 \times 10^4 \quad \text{for } y_2 < -2{\cdot}0 \times 10^{-4},$$

$$K_{in} = 1{\cdot}5128 \times 10^4 \quad \text{for } -2{\cdot}0 \times 10^{-4} < y_2 < 3{\cdot}0 \times 10^{-4},$$

$$K_{out,right} = 2{\cdot}1330 \times 10^4 \quad \text{for } y_2 > 3{\cdot}0 \times 10^{-4}.$$

The region between the two dashed lines in Figure 9 will be called the inner region, the other two regions being called the left and right outer regions. The width of the inner region is 0·5 mm, i.e., equal to δ but the region is not centred around zero. The inner stiffness, i.e., the stiffness between the two dotted lines, K_{in}, is very close to the linear stiffness, while the outer stiffnesses are between 26 and 41% higher than the inner stiffness. Hence, the non-linear function is given by

$$N_2(y_2) = \begin{cases} 1{\cdot}9047 \times 10^4 y_2 + 0{\cdot}7837 & \text{if } y_2 < -2{\cdot}0 \times 10^{-4}, \\ 1{\cdot}5128 \times 10^4 y_2 & \text{if } -2{\cdot}0 \times 10^{-4} < y_2 < 3{\cdot}0 \times 10^{-4}, \\ 2{\cdot}1330 \times 10^4 y_2 - 1{\cdot}8607 & \text{if } y_2 > 3{\cdot}0 \times 10^{-4}. \end{cases} \tag{13}$$

With equation (13), a complete set of identified equations of motion is obtained. The inner stiffness of the bilinear function is essentially the linear stiffness hence it can be moved to

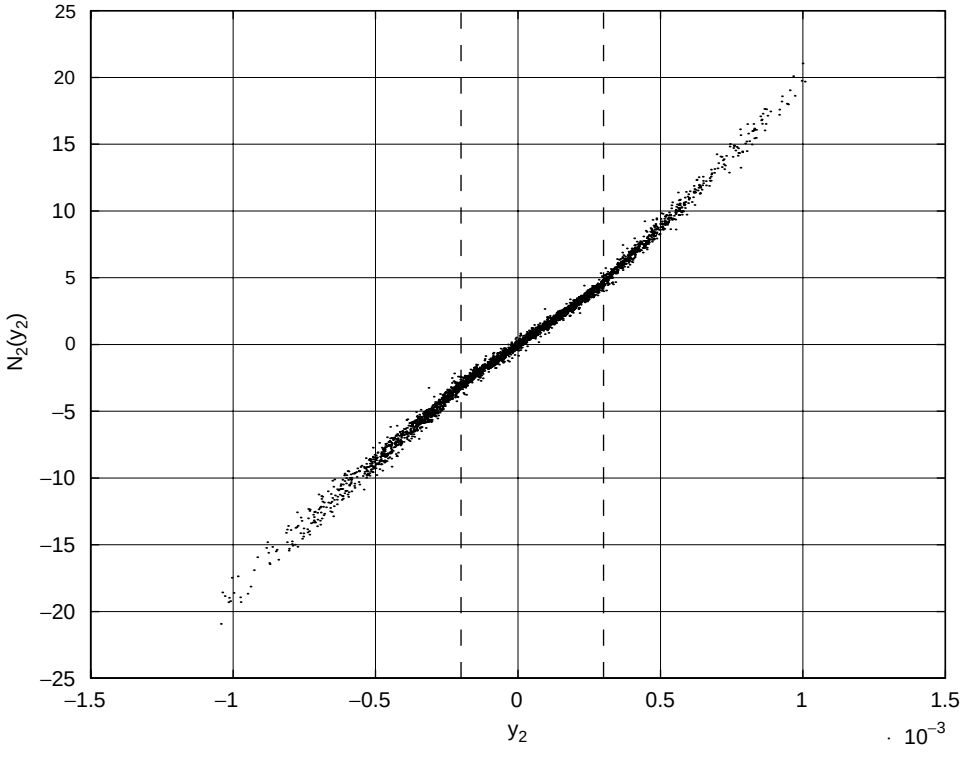

Figure 9. $N_2(y_2)$ (N) against y_2 (m) for system with freeplay stiffness, $\delta = 0{\cdot}5$ mm.

the stiffness matrix, yielding

$$\begin{bmatrix} 1 & 0 \\ 0 & 1 \end{bmatrix} \begin{Bmatrix} \ddot{y}_1 \\ \ddot{y}_2 \end{Bmatrix} + \begin{bmatrix} 2{\cdot}7564 & -0{\cdot}4500 \\ -0{\cdot}4791 & 3{\cdot}6802 \end{bmatrix} \begin{Bmatrix} \dot{y}_1 \\ \dot{y}_2 \end{Bmatrix} + 10^4 \begin{bmatrix} 1{\cdot}0833 & -0{\cdot}3180 \\ -0{\cdot}2810 & 1{\cdot}5128 \end{bmatrix} \begin{Bmatrix} y_1 \\ y_2 \end{Bmatrix}$$
$$+ \begin{Bmatrix} 0 \\ \begin{cases} 0{\cdot}3917 \times 10^4 y_2 + 0{\cdot}7837 & \text{if } y_2 < -2{\cdot}0 \times 10^{-4} \\ 0 & \text{if } -2{\cdot}0 \times 10^{-4} < y_2 < 3{\cdot}0 \times 10^{-4} \\ 0{\cdot}6202 \times 10^4 y_2 - 1{\cdot}8607 & \text{if } y_2 > 3{\cdot}0 \times 10^{-4} \end{cases} \end{Bmatrix} = \begin{Bmatrix} 0{\cdot}3472 w_1(t) \\ 0{\cdot}3288 w_2(t) \end{Bmatrix}. \tag{14}$$

The system described by these equations is very close to the actual experimental system, as can be seen from Figure 11, where the acceleration responses of the experimental system and the identified equations of motion to the same forcing signal are plotted against time. The agreement between the two responses is very good.

For the $\delta = 1{\cdot}05$ mm case, the force–displacement plot of Figure 10 shows the same picture as that of Figure 9, the main difference being that the distance between the dotted lines is 1·05 mm. Again, the inner region is not centred and there are three stiffnesses, given by

$$\begin{aligned} K_{out,left} &= 1{\cdot}9994 \times 10^4 \quad \text{for } y_2 < -5{\cdot}0 \times 10^{-4}, \\ K_{in} &= 1{\cdot}5285 \times 10^4 \quad \text{for } -5{\cdot}0 \times 10^{-4} < y_2 < 5{\cdot}5 \times 10^{-4}, \\ K_{out,right} &= 2{\cdot}1850 \times 10^4 \quad \text{for } y_2 > 5{\cdot}5 \times 10^{-4}. \end{aligned}$$

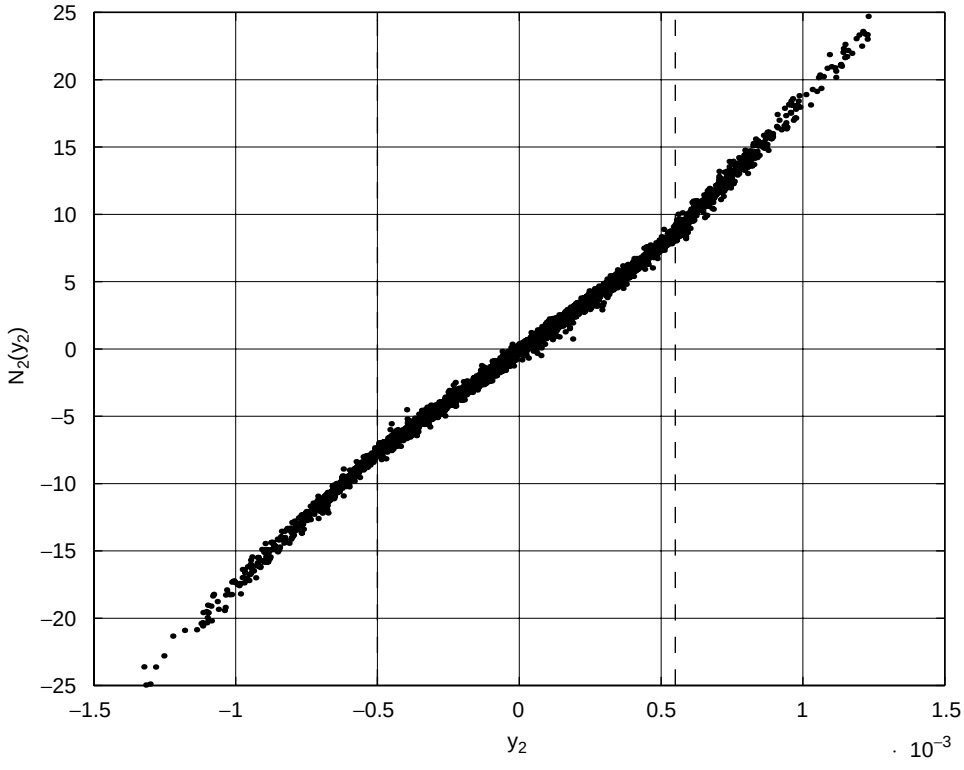

Figure 10. $N_2(y_2)$ (N) against y_2 (m) for system with freeplay stiffness, $\delta = 1{\cdot}05$ mm.

Note that all three stiffness values are approximately equal to the values obtained for the $\delta = 0{\cdot}5$ mm case. This is logical since the only difference between the two cases is the width of the bilinear region; the stiffnesses are unchanged. The non-linear function for the $\delta = 1{\cdot}05$ mm case could then be expressed as

$$N_2(y_2) = \begin{cases} 1{\cdot}9994 \times 10^4 y_2 + 2{\cdot}4574 & \text{if } y_2 < -5{\cdot}0 \times 10^{-4}, \\ 1{\cdot}5285 \times 10^4 y_2 & \text{if } -5{\cdot}0 \times 10^{-4} < y_2 < 5{\cdot}5 \times 10^{-4}, \\ 2{\cdot}1850 \times 10^4 y_2 - 3{\cdot}4083 & \text{if } y_2 > 5{\cdot}0 \times 10^{-4}. \end{cases} \tag{15}$$

Again, using equation (15), a complete set of identified equations of motion can be obtained, again by moving the inner stiffness to the stiffness matrix

$$\begin{bmatrix} 1 & 0 \\ 0 & 1 \end{bmatrix} \begin{Bmatrix} \ddot{y}_1 \\ \ddot{y}_2 \end{Bmatrix} + \begin{bmatrix} -2{\cdot}7471 & -0{\cdot}6596 \\ -0{\cdot}6093 & -3{\cdot}8485 \end{bmatrix} \begin{Bmatrix} \dot{y}_1 \\ \dot{y}_2 \end{Bmatrix} + 10^4 \begin{bmatrix} -1{\cdot}1006 & -0{\cdot}3121 \\ -0{\cdot}2795 & -1{\cdot}5285 \end{bmatrix} \begin{Bmatrix} y_1 \\ y_2 \end{Bmatrix}$$
$$+ \begin{Bmatrix} 0 \\ \begin{cases} 0{\cdot}4709 \times 10^4 y_2 + 2{\cdot}4574 & \text{if } y_2 < -5{\cdot}0 \times 10^{-4} \\ 0 & \text{if } -5{\cdot}0 \times 10^{-4} < y_2 < 5{\cdot}5 \times 10^{-4} \\ 0{\cdot}6565 \times 10^4 y_2 - 3{\cdot}4083 & \text{if } y_2 > 5{\cdot}5 \times 10^{-4} \end{cases} \end{Bmatrix} = \begin{Bmatrix} 0{\cdot}3486 w_1(t) \\ 0{\cdot}3303 w_2(t) \end{Bmatrix}.$$

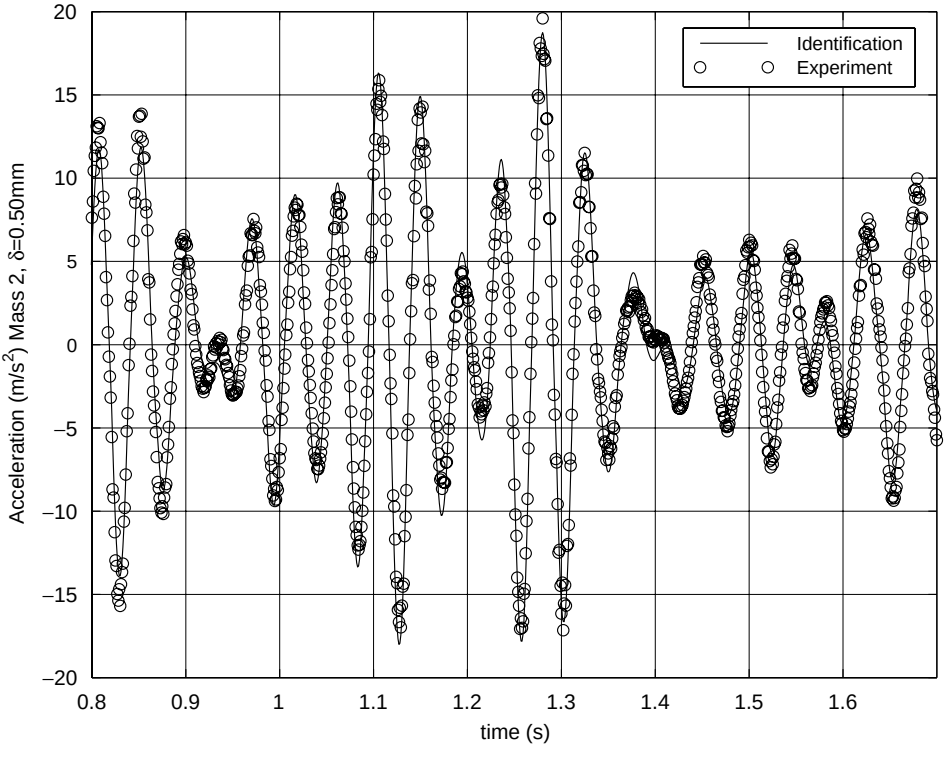

Figure 11. Comparison of experimental and identified responses for system with bilinear stiffness, $\delta = 0{\cdot}5$ mm. ——, Identification; ○—○, experiment.

The system described by these equations is also very close to the actual experimental system, as can be seen in Figure 12 where the acceleration responses of the real and identified systems to the same forcing signal are plotted against time. The agreement between the two responses is clearly very good.

4. CONCLUSIONS

In this paper, the constant level method for the identification of non-linear systems was evaluated on an experimental dynamical systems with two types of non-linearity, cubic and bilinear stiffness. The CLI method is a simple identification method that can identify both the equations of motion and the non-linear functions of systems with non-linear terms that depend on only one of the state variables. The approach was found to identify successfully the experimental system given forced response acceleration data. The cases that were identified included a linear case, a case with cubic stiffness and two cases with bilinear stiffness. In all cases, the identified equations of motion were numerically integrated and the resulting responses were compared to the measured responses, yielding very good agreement. It was concluded that the CLI technique is a very effective method for identifying both continuous and discontinuous non-linearities. Further work will concern the experimental validation of the method on more complex systems with many degrees of freedom.

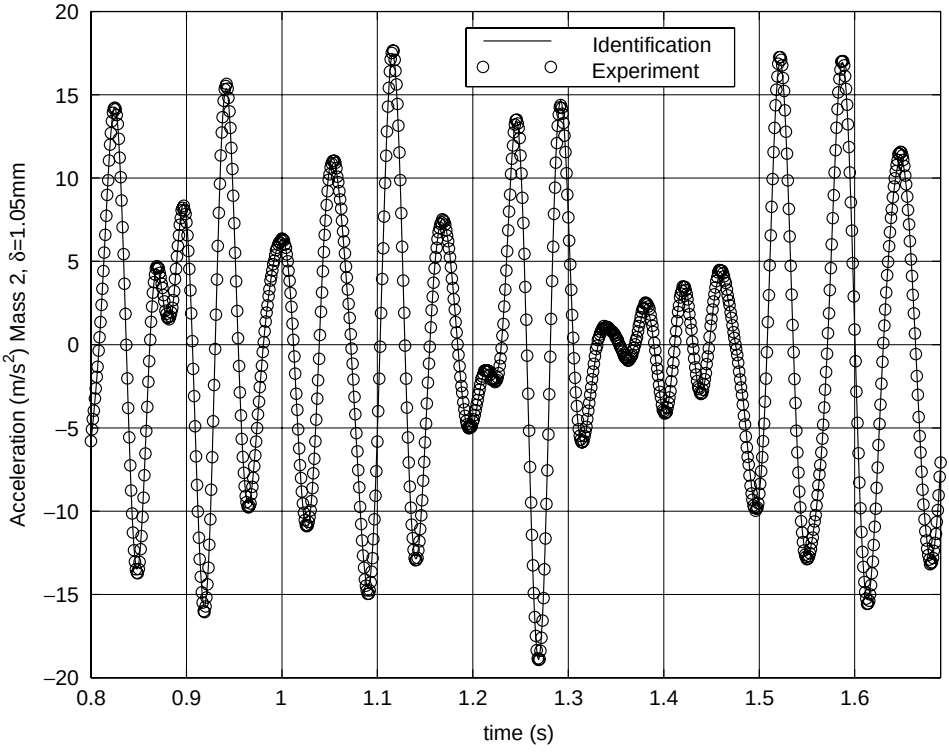

Figure 12. Comparison of experimental and identified responses for system with bilinear stiffness, $\delta = 1{\cdot}05$ mm. ——, Identification; ○—○, experiment.

ACKNOWLEDGMENTS

The author would like to thank Prof. J. E. Cooper for his useful advice and J. Wong, F. Geracci and G. Vio for their help with the experimental measurements.

REFERENCES

1. S. Chen and S. A. Billings 1989 *International Journal of Control* **49**, 1013–1032. Representations of non-linear systems: the NARMAX model.
2. G. Palm and B. Pöpel 1985 *Quarterly Review of Biophysics* **18**, 135–164. Volterra representation and Wiener-like identification of nonlinear systems: scope and limitations.
3. M. Simon and G. R. Tomlinson 1984 *Journal of Sound and Vibration* **96**, 421–436. Use of the Hilbert transform in modal analysis of linear and non-linear structures.
4. K. Worden and G. R. Tomlinson 2001 *Nonlinearity in Structural Dynamics*. Detection, Identification and Modelling. Bristol and Philadelphia: Institute of Physics Publishing.
5. E. F. Crawley and A. C. Aubert 1986 *American Institute of Aeronautics and Astronautics Journal* **24**, 155–162. Identification of nonlinear structural elements by force-state mapping.
6. K. Worden and G. R. Tomlinson 1994 *Mechanical Systems and Signal Processing* **8**, 319–356. Modelling and classification of nonlinear systems using neural networks. I: simulation.
7. V. Lenaerts, G. Kershen and J.-C. Golinval 2001 *Journal of Sound and Vibration* **244**, 597–613. Theoretical and experimental identification of a nonlinear beam.

8. M. Ajjan Al-Hadid and J. R. Wright 1990 *Mechanical Systems and Signal Processing* **4**, 463–482. Application of the force-state mapping approach to the identification of non-linear systems.
9. M. Ajjan Al-Hadid and J. R. Wright 1992 *Mechanical Systems and Signal Processing* **6**, 383–401. Estimation of mass and modal mass in the identification of non-linear single and multi degree of freedom systems using the force-state mapping approach.
10. K. Worden 1989 *Ph.D. Thesis, Department of Mechanical Engineering, Heriot-Watt University*. Parametric and nonparametric identification of nonlinearity in structural dynamics.
11. G. Dimitriadis and J. E. Cooper 1998 *Proceedings of the Institute of Mechanical Engineers, Part G* **212**, 287–298. A method for identification of non-linear multi-degree-of-freedom systems.
12. W. G. Luber 1997 *Proceedings of the CEAS International Forum on Aeroelasticity and Structural Dynamics*, *Rome*, *Italy*, 173–182. Flutter prediction on a combat aircraft involving backlash and actuator failures on control surfaces.
13. N. E. King 1994 *Ph.D. Thesis, School of Engineering, University of Manchester*. Detection of structural nonlinearity using Hilbert transform procedures.